



Cite this: DOI: 10.1039/d4dt03428g

# Polyoxometalate-based materials in therapeutic and biomedical applications: current status and perspective

Milad Moghadasi, Mohammad Abbasi, Mahtab Mousavi and Masoud Mirzaei  \*

An increasing number of studies have demonstrated that polyoxometalate-based materials have biological applications, which means that polyoxometalate species have potential in medicine. The antibacterial, antiviral, and anticancer properties of polyoxometalates make them promising candidates for a new generation of metallodrugs in treating diseases due to their versatile structures, unique physicochemical properties, and easy synthesis processes. Recent studies have focused on the use of these materials as chemotherapeutic and photothermal agents with the capacity to generate reactive oxygen species and on the study of their mechanisms. However, due to the high solubility and long-lasting toxicity effects of pure polyoxometalates, their modification with heterometals, organic molecules, and interactions with biomolecules is an efficient strategy for introducing them into biological media and can be considered a key issue of the bioorthogonal chemistry of polyoxometalates. Here, we summarize and discuss the current status of biomedical applications of polyoxometalate-based materials. Furthermore, the prospect of using these materials for therapeutic purposes is anticipated, indicating promising directions for future research and development.

Received 10th December 2024,  
Accepted 17th February 2025

DOI: 10.1039/d4dt03428g

rsc.li/dalton

## 1. Introduction

Although therapeutic strategies have been developed and improved nanomaterials are employed in medicine, their effectiveness without side effects is still insufficient. Therefore, the development and improvement of strategies and nanomaterials is still needed.<sup>1</sup> Polyoxometalates (POMs) are a diverse class of nanoscale anionic clusters made from metals and oxygen which have substantial negative charge densities and contain various transition metals such as Mo, W, V, Nb, Ta, Ge, *etc.* The adjustable acidity and solubility of POMs make them useful catalysts in the execution of numerous organic reactions. In addition, the activity of POMs can be controlled by adjusting their constituent elements and optimizing their acidic and multi-electron redox properties for specific reaction conditions.<sup>2,3</sup>

The construction of POM-based materials through the integration of POMs with organic/inorganic fragments allows for the expansion of their applications within materials science and nanotechnology. The synergistic effect of these materials leads to various applications, including catalysis,<sup>4</sup> medicine,<sup>5–7</sup> electrochemical processes,<sup>8</sup> analytical sample preparation,<sup>9</sup> and magnetic<sup>10</sup> applications. Importantly, the unique prop-

erties of POMs require ongoing investigation within the biomedical sciences, highlighting their potential to drive significant innovations in drug delivery systems, new therapeutic interventions, and biosensing technologies.<sup>11,12</sup>

Their potent enzyme-like activity enables the regulation of reactive oxygen species (ROS) within the body, facilitating the treatment of tumors and inflammation. Additionally, these materials demonstrate commendable mechanical characteristics, making them a suitable medium for drug encapsulation and delivery, while concurrently acting as effective enzyme carriers to improve therapeutic interventions.<sup>13</sup>

Although numerous review articles on POM-based materials in medicine and biological applications have recently been published,<sup>5–7,11</sup> the present study briefly highlights the latest investigations, current biomedical applications, and the effectiveness of POM-based materials, with inorganic biochemistry insight.

## 2. Biomedical applications

### 2.1. Biosensing

Currently, there is a growing emphasis on diagnostic procedures within clinical methods being quick, precise, low-priced, and uncomplicated. Due to their excellent sensitivity, simplicity, and ease of use, electrochemical and chemilumi-

Department of Chemistry, Faculty of Science, Ferdowsi University of Mashhad, Mashhad 9177948974, Iran. E-mail: mirzaesh@um.ac.ir

nescence (CL) methods are becoming indispensable tools in clinical diagnostics. Exhibiting remarkable electron affinity and excellent multi-electron redox ability, POMs are likely to emerge as promising materials for the development of electrochemical and CL sensors.<sup>14</sup>

Herein, a new carbon-based sensing material with multi-component active centers was synthesized by the modification of basket-type POMs. The  $\text{CoP}_6\text{Mo}_{18}\text{@NiO-CNF}$  sensor showed excellent sensitivity to L-tryptophan (L-Trp) and dopamine (DA). The specific structure of POMs, especially the  $\{\text{CoP}_6\text{Mo}_{18}\text{O}_{73}\}$  basket-type POM, improved the electrochemical performance of the sensor due to increasing surface oxygen atoms and enabling mixed-valence  $\text{Mo(V)}/\text{Mo(VI)}$  states. The integration of POMs with NiO-loaded carbon nanofibers

(NiO-CNF) greatly increased the conductivity, selectivity, and stability of the developed probe, yielding a more robust current response toward target analytes. This nanocomposite has great potential for applications related to electrochemical sensing because of its excellent redox properties and its promotion of electron transfer. In addition, parallel and repeated experiments showed that biosensors have strong stability and exceptional repeatability in the biological environment, such that the relative standard deviation (RSD) values of DA and L-Trp were 1.03% and 1.12%, respectively.<sup>15</sup>

Among the various types of POMs, Keggin-type POMs possess strong electron-accepting abilities, making them ideal for biosensing applications.<sup>16</sup> Therefore, an innovative Keggin-type POM-based nanozyme,  $[\text{H}_7\text{SiW}_9\text{V}_3\text{O}_{40}(\text{DPA})_3]\cdot 4\text{H}_2\text{O}$  ( $\text{SiW}_9\text{V}_3/\text{DPA}$ ) (DPA; dipyridylamine), was proposed as a highly efficient probe for the sensitive determination of the antibiotic kanamycin (KAN).  $\text{SiW}_9\text{V}_3/\text{DPA}$  exhibits laccase-mimicking activity with increased resistance against degradation compared to the natural laccase. This interaction involves positively charged KAN and negatively charged  $\text{SiW}_9\text{V}_3$  particles that induce chromogenic reactions. The resultant red products indicate the existence of KAN. However, as the concentration of KAN increased in the detection process, the red color faded gradually. In the reusability test, the laccase-mimicking activity remained at 81.7% after five cycles. The stability test also showed a 92.8% performance even after 30 days of storage at 25 °C. Based on these results, this biosensor has exceptional stability and reusability.<sup>17</sup>

In another approach, a Keggin-type POM was applied to a POM-hydrogel-based CL system that represents a simple and powerful means of developing sustainable luminescence emission. By incorporating the peroxidase (POD)-mimicking nanozyme POM and the bioenzyme glucose oxidase (GOx) within the hydrogel matrix, a strong CL response based on diffusion-controlled catalysis and cascade reactions is generated. The use of Keggin-type POM promotes the decomposition of calcium carbonate ( $\text{CaCO}_3$ ) and strengthens the interaction between luminol and hydrogen peroxide ( $\text{H}_2\text{O}_2$ ), resulting in light emission. Correspondingly, this system exhibits very good reproducibility and storage stability, in generating glow-type CL, with a good RSD of less than 2.4% after 10 cycles. It also maintains a stable glow-type feature even after storage at 4 °C for several days. Considering these features, the POM-hydrogel-based CL system holds great promise for glucose detection in human serum samples with high efficiency and excellent accuracy.<sup>18</sup>

In biosensing procedures, POMs are used in heterojunction systems to enhance sensitivity and selectivity. This synergistic system enables better control of electronic and optical properties, improving detection sensitivity and stability in sensors for biomolecules like glucose, DNA, or proteins. As a result, a POM-based heterojunction nanocomposite ( $\text{GdP}_5\text{W}_{30}\text{O}_{110}\text{@WS}_2$ ) was prepared with intrinsic and stable POD-like catalytic activities under harsh conditions. These nanoclusters can oxidize chromogenic substrates in the presence of  $\text{H}_2\text{O}_2$ , producing colored products that can be quanti-



**Masoud Mirzaei**

*Masoud Mirzaei received his Ph. D. in Inorganic Chemistry at Ferdowsi University of Mashhad (FUM), where he is currently working as a distinguished professor. His interdisciplinary research is at the interface of inorganic chemistry and materials science. His work focusses on the fundamental science and applications of metal cluster-based complexes and materials such as polyoxometalates (POMs) and metal-organic frameworks*

*(MOFs). Their prospective uses include medical, energy, and environmental applications. His laboratory in FUM creates polyoxometalate-based frameworks, by using covalent and non-covalent interactions in creating open framework materials for specific applications like gas storage and separation, drug detection, and catalysis. He has published more than 240 ISI cited papers, including reviews and two books with Elsevier and the Royal Society of Chemistry. He was the President of the Ferdowsi University of Mashhad (FUM) whose mission is to help talents flourish and find solutions to real life problems by developing science-based firms (4th generation university). Also, he has been the Chairman of the Zeolite and Porous Materials Committee of the Iranian Chemical Society since 2017 and the President of Khorasan Science and Technology Park (KSTP) and served as the Associate Editor of Inorganic Chemistry Research, a monthly open access journal published by the Iranian Chemical Society. He has received funds and awards for research and leadership from the Iran National Science Foundation (INSF), Iran Science Elites Federation (ISEF), and the Academy of Sciences of the Islamic Republic of Iran. In 2021, 2023, and 2024, Professor Mirzaei was ranked among the top 1% International highly cited Scientists by ESI (Web of Science). He was named distinguished professor of inorganic chemistry in 2022. He served as an Editorial Board member of Polyhedron and Journal of the Iranian Chemical Society.*

tatively measured. The mechanism includes the generation of reactive hydroxyl radicals ( $\cdot\text{OH}$ ) by  $\text{GdP}_5\text{W}_{30}\text{O}_{110}$ , which is indispensable for the oxidation of tetramethylbenzidine (TMB) substrates. Such outstanding catalytic performance enables the establishment of a sensitive analytical platform for the determination of  $\text{H}_2\text{O}_2$ , glutathione (GSH), and glucose using an easy TMB colorimetric method.<sup>19</sup>

As another example, a novel POM/sulfide-gated system ( $\text{H}_3\text{PW}_{12}\text{O}_{40}/\text{ZnIn}_2\text{S}_4$ ) exhibited light-harvesting and enzyme-like properties which enabled unique on-off photoelectrochemical transistor operation (Fig. 1a). It also allows for highly effective detection of miRNA-21 to activate the CRISPR/Cas13a system for genetic engineering by the generation of  $\text{H}_2\text{O}_2$  through a reaction of DA catalyzed by  $\text{PW}_{12}$  species. The separation of charge carriers induced by  $\text{PW}_{12}$  at the heterojunction interface leads to a pronounced gating effect-inhibited organic photoelectrochemical transistor (OPECT) operation upon DA polymerization to polydopamine (PDA). PDA acts as a quencher and thus changes sensor operation, enabling sensitive detection of miRNA-21 (Fig. 1b). This sensor showed acceptable recoveries of 92.59%–100.32% during actual sample testing, which implies that it has good reproducibility in measurement and hence is consistent in different analyses. The inclusion of CRISPR/Cas13a within the OPECT sensor has great potential for practical medical diagnostics, potentially aiding in the early detection of certain diseases.<sup>20</sup>

Such findings highlight not just a scientific breakthrough but also offer a glimpse into the elegant complexities within

POM-based systems. Moreover, future exploration into these systems promises breakthroughs in biosensor performance, particularly as novel integration techniques with nanoscale and multifunctional materials pushing the boundaries of detection precision and reliability across biomedical applications.

Compared with POM-based materials, the utilization of metal–organic frameworks (MOFs) for biosensing applications has attracted much research attention and they have been recognized as among the best candidates. However, the poor conductivity nature of many MOFs as electrochemical biosensors is a significant concern.<sup>21</sup> For this reason, the development of conductive MOFs, the improvement of conductivity in MOFs using species such as POMs, and the formation of POM–MOF composites/hybrids can be effective in the development of efficient biosensors.<sup>22</sup>

Due to the improved conductivity and biocompatibility and the possibility of structural diversity in MOF composites, they can have wide applications in the detection of biomolecules. Several reports show that MOF-based biosensors that contain bioreceptors are highly sensitive and selective. Bioreceptors, such as nucleic acids, peptides, enzymes, antibodies, *etc.*, can expand the biosensing platform through encapsulation, immobilization, and adsorption. Bioreceptor attachment to MOFs *via* non-covalent interactions may result in shedding; although there are many covalent attachment methods for bioreceptors to MOFs, ensuring receptor attachment to MOFs' specific sites remains a challenge. The presence of POMs in these platforms

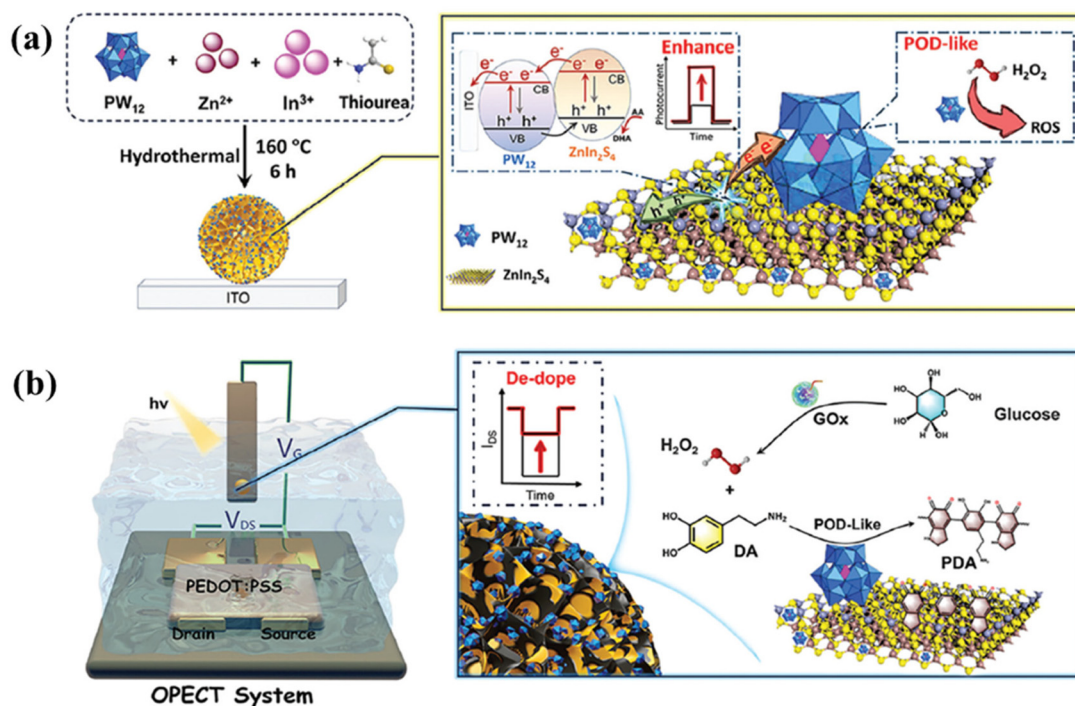


**Fig. 1** (a) Representation of fabrication of the  $\text{PW}_{12}/\text{ZnIn}_2\text{S}_4$  heterojunction and POD-like activity improvement by  $\text{PW}_{12}$  at the heterojunction interface. (b) Schematic illustration of the *in situ* catalytic conversion of DA into PDA and sensitivity of the OPECT response for target sensing. Adapted with permission from ref. 20. Copyright 2024 Wiley.

can also be very helpful due to their key role in establishing diverse non-covalent interactions with bioreceptors.<sup>23</sup>

It should be noted that stability and biocompatibility are among the most important challenges in MOF-based biosensors. Although synthesized MOFs based on metals such as copper (Cu), calcium (Ca), zinc (Zn), iron (Fe), and magnesium (Mg) are mostly biocompatible and suitable for molecular sensing, they do not have the necessary stability. In this regard, the use of MOF-based composites such as POM@MOF can also provide desirable stability and sensitivity in addition to conductivity.<sup>24</sup>

## 2.2. Biomedical therapies

In general, POM-based materials for therapy should exhibit POD-like activity. The exposure of the body to noxious stimuli can sometimes lead to depletion of endogenous ROS, thereby causing an imbalance between oxidative and antioxidant processes, ultimately contributing to tissue injury. These materials possess the unique ability to provide  $\text{H}_2\text{O}_2$  and sufficient ROS. This property allows for the degradation of DNA molecules, resulting in a defensive mechanism and the regulation of ROS levels within the body.<sup>5,13</sup>

Using POM-based MOFs as antibacterial agents in non-antibiotic treatment methods has gained interest. The disadvantages such as the low efficiency of ROS generation and the high concentration of metal ions released in this method led

to the design and synthesis of emerging materials to eradicate bacteria and improve wound healing. For instance, encapsulation of three Keggin-type anions ( $\text{SiW}_{12}\text{O}_{40}^{4-}$ ,  $\text{PW}_{12}\text{O}_{40}^{3-}$ , and  $\text{PMo}_{12}\text{O}_{40}^{3-}$ ) along with  $\text{Cu(II)}$  as the counter ion into HKUST-1 pores, which was coated with a surfactant ( $\text{CuPOM-MOF@S}$ ), was reported as a catalytic reservoir for cascaded ROS generation against *Escherichia coli* (*E. coli*) and *Staphylococcus aureus* (*S. aureus*) bacteria (Fig. 2a). Compared to the control group, the fluorescence intensities of groups treated with  $\text{CuPOM-MOF@S}$  showed remarkable enhancement, indicating improved permeability of the outer membrane (Fig. 2b). In addition, the rise in OD (420 nm) values implied enhanced permeability in the inner membrane. As a result, the interactions between the hybrid and bacterial membranes caused permeation into the outer and inner membranes, leading to alterations in membrane morphology (Fig. 2c and d). The findings of this study showed that the presence of highly negatively charged POMs facilitated the retention of elevated concentrations of catalytic  $\text{Cu(II)}$  ions within the framework through strong electrostatic interactions. The cytotoxic potential of  $\text{CuPOM-MOF@S}$  was evaluated through *in vitro* studies employing human umbilical vein endothelial cells (HUVECs) and human immortalized keratinocytes (HaCaT). At a concentration of  $20 \mu\text{g mL}^{-1}$ ,  $\text{CuPOM-MOF@S}$  maintained the viability of over 70–90% of HUVECs and HaCaT cells. Results of live/dead cell staining indicated that the cells exhibited well-

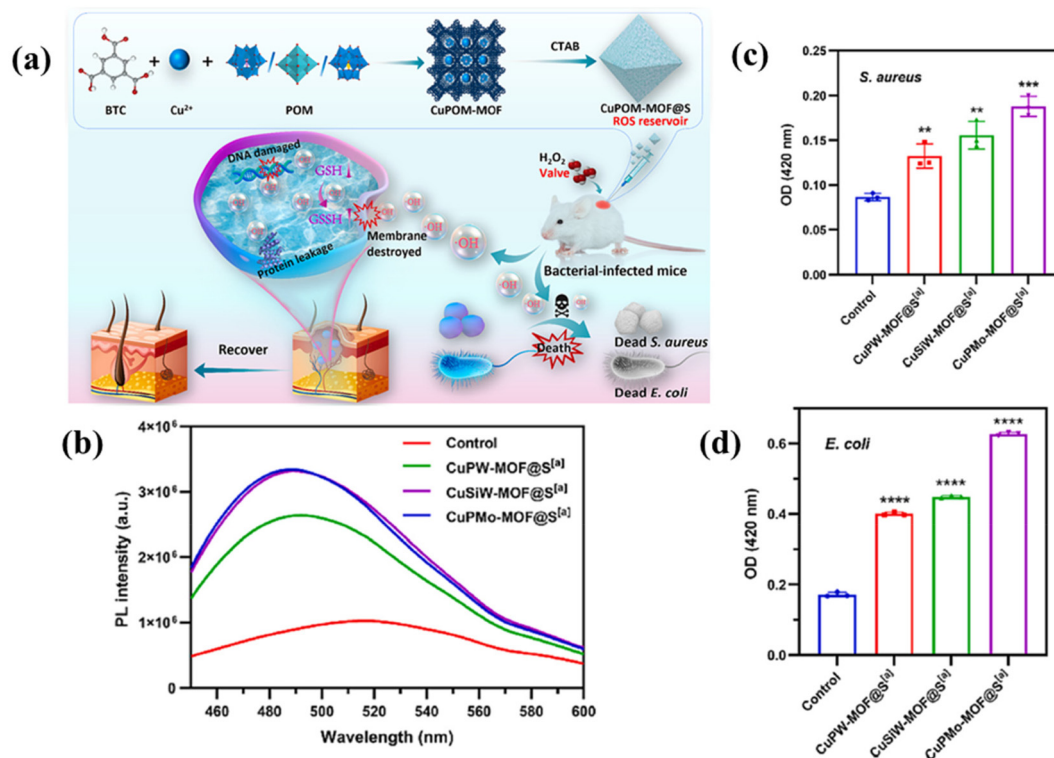


**Fig. 2** (a) A schematic representation outlining the preparation of the  $\text{CuPOM-MOF@S}$  hybrid, its antibacterial activity, and its therapeutic potential for bacterial infections. (b) Photoluminescence spectra of  $\text{CuPOM-MOF@S}$  hybrids in comparison with the control group. (c and d) The synthesized hybrids' influence on permeability within *S. aureus* and *E. coli* bacteria. Adapted with permission from ref. 25. Copyright 2023 Elsevier.



proliferation in the presence of CuPOM-MOF@S, demonstrating the biocompatibility in normal skin tissues.<sup>25</sup>

POMs can also improve radiodynamic therapy (RDT) under hypoxic conditions. For example, a super tetrahedral POM cluster,  $K_{21}Na_8[KFe_{12}(OH)_{18}(\alpha-1,2,3-P_2W_{15}O_{56})_4]\cdot 70H_2O$  (called  $Fe_{12}$ -POM), was developed which consisted of four  $P_2W_{15}$  units acting as X-ray energy antennas, transferring energy to the  $Fe_3$  core as an energy and electron receptor. Additionally, the  $Fe_3$  core functioned as a catalytic center. Transfer of an X-ray-activated electron from W in  $P_2W_{15}$  to  $Fe(III)$  in the  $Fe_3$  core resulted in the transformation of  $Fe(III)$  to  $Fe(II)$ , which led to the occurrence of a highly effective Fenton reaction that acted as a catalyst for the conversion of  $H_2O_2$  to  $\cdot OH$ . Under X-ray radiation, a metal-to-metal charge transfer (MMCT) phenomenon occurs between  $P_2W_{15}$  and the  $Fe_3$  core and a remarkable 139-fold increase in  $\cdot OH$  generation compared to  $Fe_{12}$ -POM alone (Fig. 3a). The rapid emergence of the  $\cdot OH$  species could potentially induce cancer immune cell death (ICD), reprogram the immune environment, and enhance the anticancer immune response (Fig. 3b). In this study,  $Fe_{12}$ -POM showed significant antitumor activity towards 4T1 tumor cells with an  $IC_{50}$  value of 123.2  $\mu M$ , six times higher than for  $Fe_{12}$ -POM alone, indicative of a significant synergistic enhancement in antitumor activity of  $Fe_{12}$ -POM under X-ray radiation.<sup>26</sup>

As another example, a Sb-rich  $\{Sb_{21}Tb_7W_{56}\}$  POM (POM-1) with nanoscale size has recently become a potential antitumor agent in cancer therapy, particularly in the treatment of non-

small cell lung cancer (NSCLC). POM-1 exerts potent antitumor effects through the induction of both apoptosis and ferroptosis in cancer cells (Fig. 4a). Cytotoxicity was reported against H1299 and A549 cells with  $IC_{50}$  values of 3.245  $\mu M$  and 3.591  $\mu M$ , respectively, and the antitumor effect of POM-1 against these lung cell lines *in vitro* showed that the dose and time of treatment had a significant role in cell inhibition (Fig. 4c-e). By triggering mitochondrial damage and activating the p53 signaling pathway, POM-1 provokes apoptosis, which thereby promotes programmed cell death. Moreover, POM-1 increases Fe accumulation and impairs cellular defenses against lipid peroxidation, leading to ferroptosis, a Fe-dependent form of cell death. In both processes, ROS generation is a prerequisite for cellular death (Fig. 4b). This new dual mechanism of action offers insight into the unique anticancer mechanisms of Sb-containing POMs and is an attractive strategy for the treatment of cancer.<sup>27</sup>

As another example, diabetic wounds, due to their hypoxic environment, are susceptible to the production of excess ROS, which prevents wound healing. Moreover, hyaluronic acid (HA), due to its ability to interact with cell surface receptors, is suitable for designing HA hydrogels. In this regard, a chronological adaptive Fe-POM@HA hydrogel was fabricated by uniformly integrating Fe-POM into HA. When the wound naturally transitions to the neutral inflammation stage, Fe-POM with  $Fe(II)/Mo(v)$  mixed valences can simultaneously alleviate oxidative stress and overcome the hypoxic microenvironment

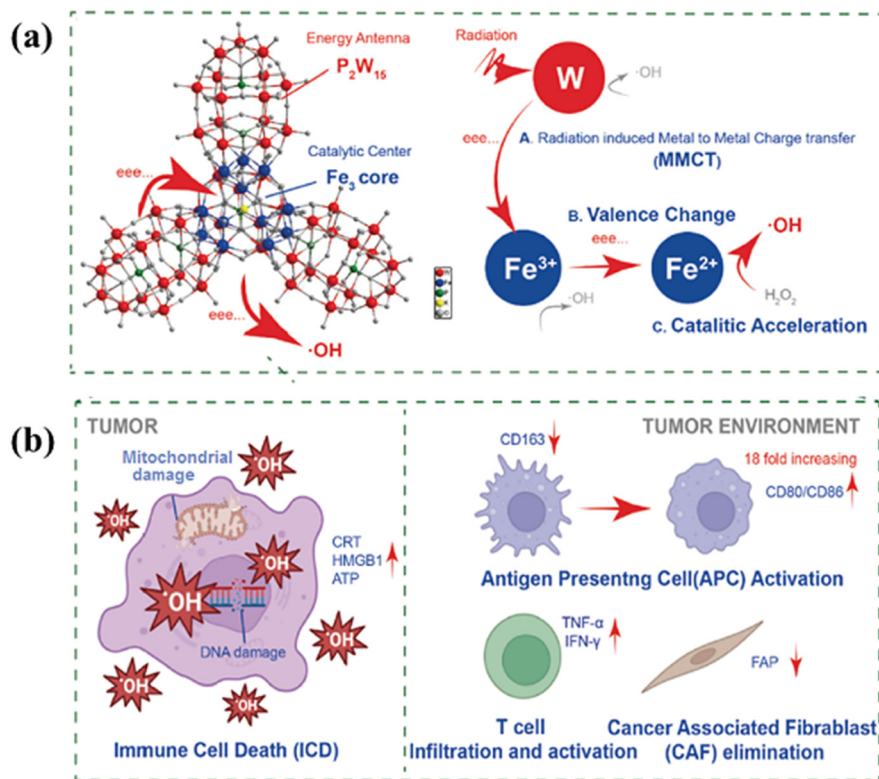


**Fig. 3** (a) Representation of the heterometallic structure based on  $Fe_{12}$ -POM. (b) Schematic illustration of the RDT process, destruction of mitochondria and DNA via ROS presence. Adapted with permission from ref. 26. Copyright 2024 ACS.

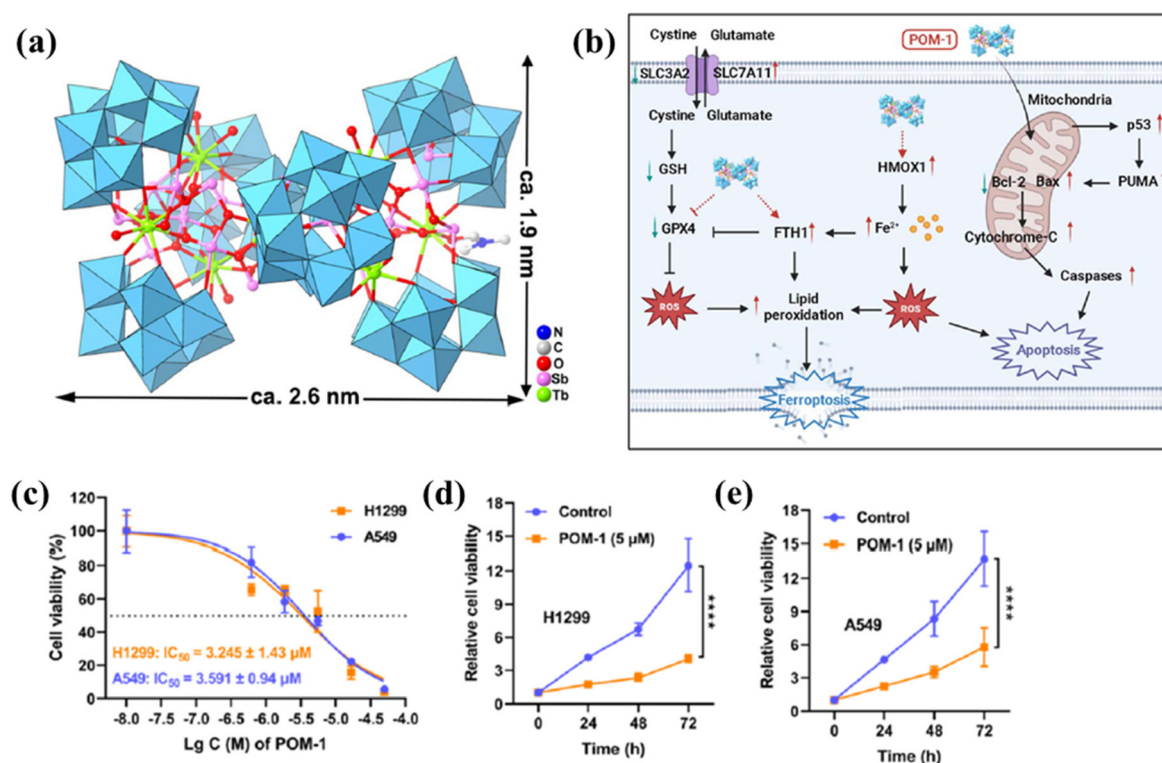


**Fig. 4** (a) Representation of the POM-1 structure. (b) The antitumor mechanism of POM-1 against NSCLC induces cell death through a combination of ferroptosis and apoptosis mechanisms. (c) Dose effects on cytotoxicity of POM-1 against cell lines. (d and e) Time-dependent cytotoxic effects of POM-1 on H1299 and A549 cell lines. Adapted with permission from ref. 27. Copyright 2024 RSC.

by continuously scavenging excessive ROS. This is due to the remarkable photochemical properties of Mo-based nanoclusters (MNCs). The facile transition between Mo(v) and Mo(vi) valence states in MNCs enhances its remarkable capability to neutralize ROS.<sup>28</sup>

Additionally, as a scaffold in skin tissue engineering, gelatin methacryloyl (GelMA), with its tunable physicochemical properties, can form chemically cross-linked bonds that enhance stability over physically cross-linked hydrogels. The excellent stability and dispersibility of MNCs would reduce their aggregation and degradation when incorporated into GelMA, thus preserving their antioxidant activity throughout their *in vivo* application. Besides, MNC-incorporated hydrogels can achieve therapeutic effects at much lower concentrations, reducing the risk of side effects associated with high concentrations of nanomaterials. In this regard, a ROS-responsive hybrid hydrogel named MNCs/GelMA was fabricated using the synergistic benefits offered by GelMA and MNCs. The micro-sized pores in MNCs/GelMA suggest the presence of a porous and interconnected network, making these hydrogels suitable for use as wound dressings. The hybrid hydrogel dressings were applied in thickness wounds of mice and showed accelerated healing times. On the seventh day, the wound area that persisted in the experimental group was approximately 1.5 times less compared with the control group and 1 time less compared with the conventional GelMA group.<sup>29</sup>

Due to their small size and limitation in near-infrared (NIR-II) absorption, MNCs are inadequate for achieving desired tumor targeting and performing NIR-II photo-thermal therapy (PTT), hindering their potential for non-inflammatory cancer treatment. Bovine serum albumin (BSA) due to its remarkable biocompatibility is a good candidate as a drug delivery system. Therefore, bifunctional nanoparticles (NPs) based on Keggin Mo-POMs and BSA (B-POM) were developed for non-inflammatory NIR-II PTT of triple-negative breast cancer (TNBC) (Fig. 5a). The interaction between POM and protein was confirmed by X-ray photoelectron spectroscopy (XPS) in which B-POM, compared to POM, shows an obviously decreased ratio of Mo(v) to Mo(vi), indicating charge transfer (CT) and chemical bond formation between Mo atoms and BSA that can also account high stability of B-POM (Fig. 5b). The presence of d-d transitions and intervalence CT in the B-POM NPs led to light absorption in the entire NIR region (Fig. 5c). Furthermore, the absorption peak near 808 nm in MNCs occurs in an almost pH-neutral environment of 6.5, as the CT from Mo(v) to Mo(vi) is responsive to the pH conditions, leading to NIR absorption (Fig. 5d). In the ROS scavenging mechanism, a larger proportion of Mo(vi) and a smaller proportion of Mo(v) can be achieved after ROS interaction. While normal tissues have a neutral pH, tumor microenvironments are characterized by their slightly acidic nature. Therefore, the enhanced NIR-II absorption of B-POM NPs

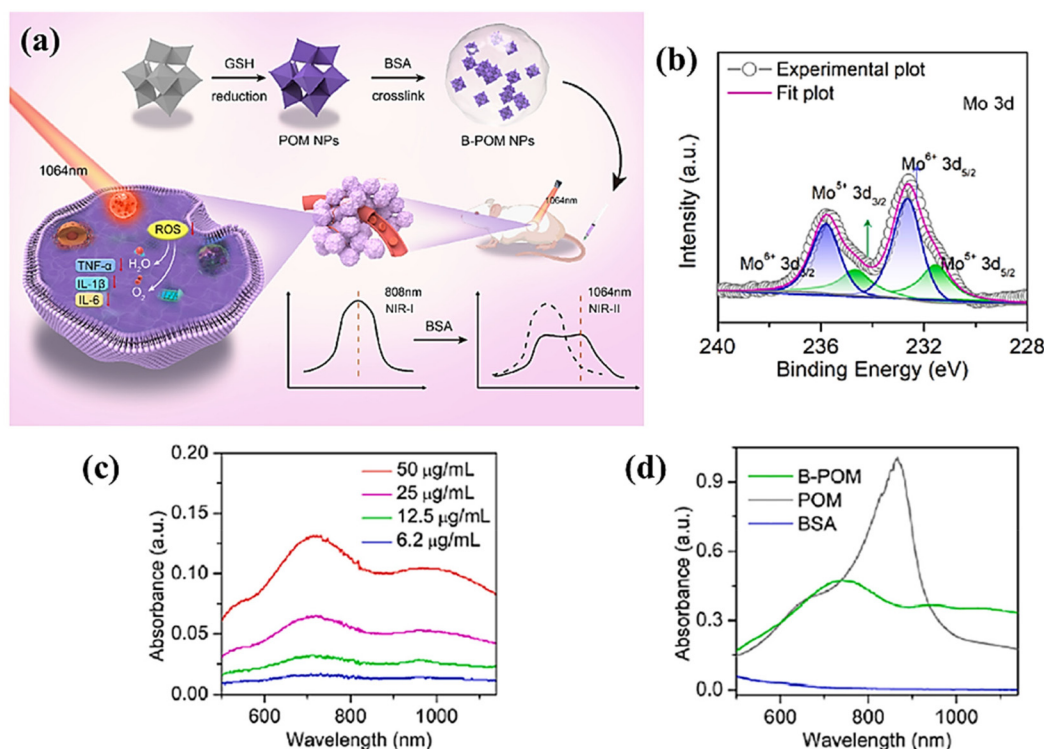


**Fig. 5** (a) Schematic representation of B-POM NPs for non-inflammatory NIR-II PTT against cancer cells. (b) High-resolution XPS spectra of the Mo 3d level for the synthesized B-POM. (c) Investigation of UV-Vis-NIR spectra of B-POM NPs at different Mo concentrations. (d) UV-Vis-NIR spectra of B-POM, POM, and BSA at pH = 6.5. Adapted with permission from ref. 30. Copyright 2024 Elsevier.

under weakly acidic conditions compared to POM makes them promising candidates for tumor NIR-II PTT treatment. In this regard, the B-POM NPs demonstrated *in vivo* high tumor inhibition efficiency under NIR-II PTT (87.0%) and excellent biocompatibility with an NIR-II photo-thermal conversion efficiency of 57.2%.<sup>30</sup>

In another study, the development of a novel route involving a Mo-based POM compound enhanced with bisphosphonate (BP) ligands possessing antitumor properties, for the synthesis of metallic gold nanostars (AuNSs), with the hybrid POM acting as both the reductant and stabilizing agent. The AuNS@POM nanocomposite contained alendronate ligands, Mo(v) ions, and Au(0) centers, increasing its targeting properties against the glioblastoma (U87) and liver cancer (MCF7) cell lines. The inclusion of BP ligands along with the oxidation of Mo(v) to Mo(vi), which transpires during AuNS fabrication, significantly enhanced the POM's antitumoral attributes. This property with NIR irradiation was strikingly enhanced, reaching almost complete cellular destruction. The IC<sub>50</sub> value of AuNS@POM against U87 within 24 hours was determined to be 47.0 μM per alendronate, both pre and post-PTT. Following a 5 day incubation period, the IC<sub>50</sub> value of U87 decreased to 32.0 μM per alendronate, while MCF7 showed an observed value of 76.0 μM per alendronate. Notably, after PTT and a subsequent 5 days of incubation, these values dramatically dropped to 7.0 μM and 6.0 μM per alendronate for U87 and

MCF7, respectively. This demonstrates a synergistic chemo- and phototherapeutic effect.<sup>31</sup>

Another area where Mo-based POMs exhibit potential is in the realm of therapeutic applications for ulcerative colitis (UC). By capitalizing on the different pH levels present in the stomach and intestines, POMs can be targeted to accumulate specifically at sites affected by UC, enhancing their therapeutic impact with heightened efficacy. Moreover, oxidative stress stands out as a pivotal factor in exacerbating inflammation and perpetuating the overproduction of ROS, representing a significant challenge in the pathophysiology of UC. Given the fundamental role ROS plays in UC progression and owing to the Mo-based POM's remarkable ability to scavenge ROS along with its sensitivity to pH fluctuations, this particular type of POM was employed as a promising agent for effectively combatting UC through ROS scavenging therapy.<sup>32</sup> On the other hand, the Mo-based NCs demonstrated significant potential as radio-protectants against X-ray irradiation and the ability to scavenge ROS, allowing for the enhancement of antioxidant enzyme activity to counter oxidative stress stemming from ionizing radiation.<sup>33</sup>

Most photothermal agents utilized in PTT are not targeted and spread without direction throughout the body, necessitating manual manipulation to achieve precision therapy. Moreover, PTT on its own falls short of eliminating tumors due to uneven heat dispersion within the tumor tissue,



leading to unavoidable tumor resurgence and metastasis. However, the highly negatively charged surface of POMs presents challenges in penetrating cell membranes; hence, carriers like MOFs are commonly employed to enhance the cellular uptake of POMs.<sup>6</sup>

The encapsulation of POMs within MOFs serves to not only augment the efficiency of cellular uptake by enhancing the surface charges of POMs but also bestow upon them a specialized activation for PTT/chemodynamic therapy (CDT) exclusively targeting tumor cells. An example is the development of an  $\text{H}_3\text{PMo}_{12}\text{O}_{40}@\text{MIL-101}$  (P@M) composite, meticulously engineered to synergistically execute PTT and CDT. The limited cellular absorption of the phosphomolybdic acid ( $\text{H}_3\text{PMo}_{12}\text{O}_{40}$ ) is rectified through confinement within MIL-101, which possesses inherent photothermal conversion capabilities and the structure of MIL-101 collapses under the acidic and reducing conditions present in the tumor micro-environment (TME), thereby facilitating the activated release of  $\text{H}_3\text{PMo}_{12}\text{O}_{40}$  specifically within tumor cells (Fig. 6). The negligible cytotoxicity of the P@M composite against the hepatocellular carcinoma (HepG2) cells was evident as cell viability remained >90% after a 48 h co-culture with concentrations up to  $1000\text{ }\mu\text{g mL}^{-1}$ . On the other hand, there were no observable destructive effects on the anatomic organ structure and P@M is a compound with high biocompatibility. The release of Fe(III) is accompanied by its concurrent reduction to Fe(II) by GSH, leading to a significant generation of  $\cdot\text{OH}$  radicals *via*

the Fenton reaction due to the elevated  $\text{H}_2\text{O}_2$  levels in the TME. Moreover, hyperthermia locally accelerates the Fenton reaction, enhancing CDT efficacy.<sup>34</sup>

Although in recent years, studies have focused on Mo-based POMs, the first organogermanium-functionalized Ge(IV)-Sb(III)-templating Dawson-like anion  $[\text{Ge}(\text{CH}_2\text{CH}_2\text{COOH})\text{SbW}_{15}\text{O}_{54}]^{12-}$  was reported with remarkable potential in photoacoustic imaging guiding PTT-CDT for breast cancer. The presence of metal sites with mixed-valence (W(V)/(VI)) and integration with Au NPs led to satisfactory tumor inhibition performance *in vivo* and lower side effects on normal tissues. Compared to HepG2 and human cervical carcinoma (HeLa) cells, this hybrid in combination with PTT-CDT demonstrated superior antitumor activity in NIR-I irradiation with an  $\text{IC}_{50}$  value of  $469\text{ }\mu\text{g mL}^{-1}$  to single CDT with an  $\text{IC}_{50}$  of  $755\text{ }\mu\text{g mL}^{-1}$ .<sup>35</sup>

In recent studies, polyoxopalladates (POPs) are used with square-planar oxo-coordinated palladium (Pd(II)) ions along with heterometals and heterogroups to initiate the apoptosis mechanism in cancer cells and can be considered as antitumor metallodrugs.<sup>36</sup> In a study, these complexes have shown promise in the preparation of antileukemic compounds with the incorporation of main group metals such as gallium (Ga(III)) and thallium (Tl(III)), inducing apoptotic cell death in leukemic cells through the generation of ROS and further activating cellular pathways of cell death. Antitumor activities of phosphate-capped 12-palladate nanocubes against human

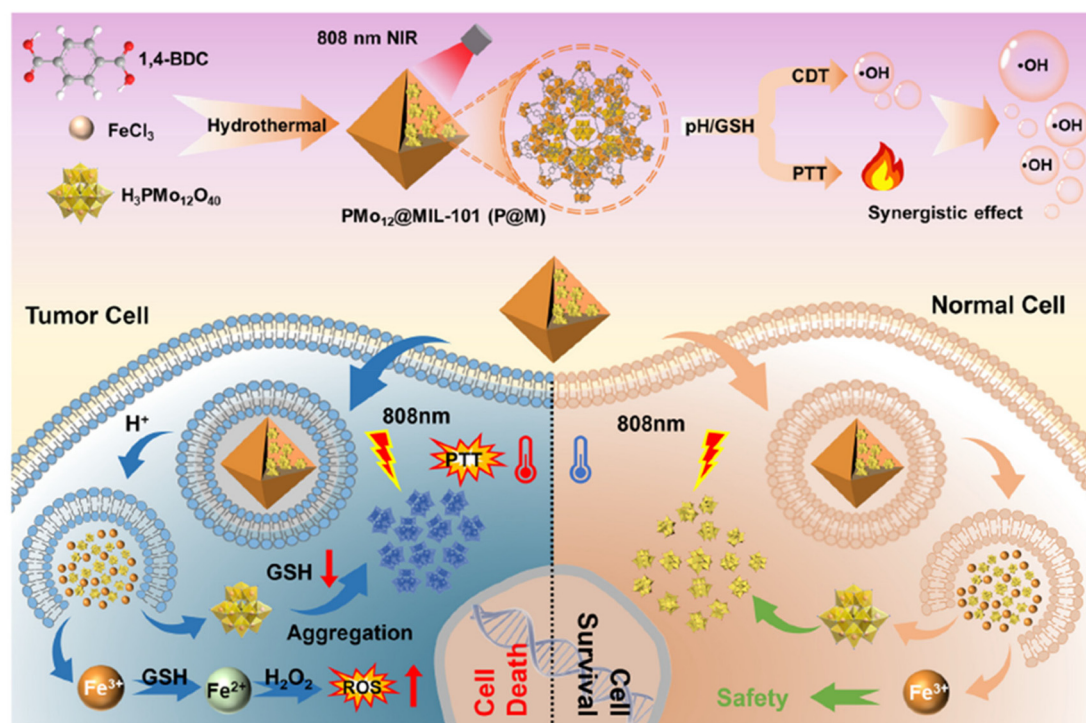


Fig. 6 Representation of illustration of  $\text{H}_3\text{PMo}_{12}\text{O}_{40}@\text{MIL-101}$  composite activity combined with PTT/CDT treatment against tumor cells. Adapted with permission from ref. 34. Copyright 2024 RSC.



melanoma and acute promyelocytic leukemia cells (HL-60) have been found for  $\text{GaPd}_{12}\text{P}_8$  and  $\text{TiPd}_{12}\text{P}_8$ , with  $\text{Ti}(\text{III})$ , forming mixed hydroxo species upon decomposition and allowing a change from neutral to acidic pH. Notably,  $\text{GaPd}_{12}\text{P}_8$  gave the lowest  $\text{IC}_{50}$  value of  $32.5\text{ }\mu\text{M}$  for HL-60 cells, while  $\text{TiPd}_{12}\text{P}_8$  showed the minimum  $\text{IC}_{50}$  value of  $25.0\text{ }\mu\text{M}$  against 518A2, thereby indicating their highest potency in these respective lines. These compounds also have shown inhibition against herpesviruses *via* the inhibition of viral replication, underlining their possible versatile therapeutic applications against different malignancies.<sup>37</sup>

POMs as alternatives to natural enzymes have great potential in mimicking enzyme activity due to their well-defined structure and tunable composition. Active catalytic sites can be intentionally introduced into POMs to obtain directional mimetic enzymes. The use of POM-based materials as artificial enzymes not only ensures high enzyme activity, but also improves specificity by introducing desired active sites, and can even emulate the catalytic functions of multiple natural enzymes simultaneously.<sup>38</sup> In this regard, an artificial metallo-protease based on sandwich  $\text{Na}_8[\text{Zr}(\text{W}_5\text{O}_{18})_2](\text{Zr}(\text{W}_5)_2)$  was synthesized for ovalbumin (OVA) amino acid hydrolysis that can be used in the proteolytic drug design. Molecular dynamics simulation showed that in the presence of surfactants, non-covalent interactions such as hydrogen bonding and van der Waals interactions between OVA and  $\text{Zr}(\text{W}_5)_2$  are established and lead to selective protein hydrolysis.<sup>39</sup>

The use of single atoms (SAs) in POMs with the aim of increasing the antioxidant effect has also been the focus of recent research. In a new study, the modification of silicotungstic acid ( $\text{H}_4\text{SiW}_{12}\text{O}_{40}$ ), with palladium (Pd) SA led to the dysfunction of hair cells (HEI-OC1) caused by neomycin in zebrafish. The findings demonstrated that a Pd SA immobilized with  $\text{H}_4\text{SiW}_{12}\text{O}_{40}$ , by mimicking the molecular structure of natural enzymes, exhibited superoxide dismutase (SOD) and catalase activity, leading to a significant increase in ROS within HEI-OC1 cells.<sup>40</sup>

POMs also exhibit the potential to overcome the limitations associated with enzyme-based nanomotors, including their vulnerability to damage. POM-nanozyme-based light-activated nanomotors are exceptionally appropriate for targeted synergistic photothermal-catalytic cancer therapy due to their intrinsic enzyme-like properties. The modification of POMotors with epidermal growth factor receptor antibodies (anti-EGFR) is advantageous for enhancing the recognition, accumulation, and infiltration of POMotors into cancer cells. In this context, the POD-like activity of the  $\text{P}_2\text{W}_{18}\text{Fe}_4$  POM-based nanomotors facilitated self-propulsion and the generation of ROS, which contributed to the cytotoxicity against tumor cells, even within the mildly acidic TME. The POMotors-EGFR + NIR group resulted in a relative cell viability of 20.6% owing to the utilization of NIR radiation with the catalytic treatment, while the POMotors and POMotors-EGFR groups showed a relative cell viability of 67.59% and 43.37%, respectively. Consequently, the therapeutic efficacy was augmented by the POMotors-EGFR, through a synergistic approach that combines enhanced tar-

geted PTT with catalytic treatment, achieving a notable tumor inhibition rate following 10 minutes of NIR irradiation.<sup>41</sup>

POMs with their adjustable acid-base and redox characteristics are appropriate as building blocks for the development of temperature-responsive POM-based materials (TRPMs) and have great potential in the development of functional nanodrugs, particularly for orthotopic brain tumor therapy. However, current POM drugs face challenges in penetrating the blood-brain barrier (BBB) and lack sufficient drug activity.<sup>42</sup> Recent studies have emphasized the self-condensation capability of POMs and the strong coordination bonds between lanthanoids (Ln) or transition metals (TMs) and lacunary POM building blocks. Despite this progress, there is a scarcity of reports on giant TM-Ln co-encapsulated POM nanoclusters with over 100 metal centers, mainly due to the difficulty in balancing the competition between TM and Ln ions in the POM system.<sup>43</sup>

Ag-based materials have shown promise as anti-tumor agents, but issues such as BBB penetration, poor tumor targeting, and low drug activity have limited their application in orthotopic brain tumors. To address these challenges, the largest and longest POM nanodrug containing Ag and Ce ions integrated into the W-O backbone was fabricated. After modifying with the brain-targeted peptide (angiopep-2-SH, Ang SH) *via* Ag-S interactions, the Ang-Te-Ag-Ce NCs exhibited superior BBB penetration and glioma-targeting capability, leading to efficient ROS activation and glioma cell death. In fact, the huge structure and space in the  $\{[\text{Ce}_{10}\text{Ag}_6(\text{DMEA})(\text{H}_2\text{O})_{27}\text{W}_{22}\text{O}_{70}][\text{B}-\alpha\text{-TeW}_9\text{O}_{33}]_9\}_2^{88-}$  (Te-Ag-Ce) NCs accommodate anticancer active centers, fluorescence imaging capability, and binding sites with peptides. Cytotoxicity experiments confirm that the synthesized Ang-Te-Ag-Ce NCs have high efficiency in inhibiting glioma (74.8%) with an  $\text{IC}_{50}$  value of  $5.66\text{ }\mu\text{M}$  *via* active sites of Ag(I) in producing ROS for cell death.<sup>44</sup>

UV light can enhance proton-coupled redox processes, and POMs are effective carriers for the photosynthesis of monodispersed metal NPs. They function as both reducing agents and stabilizers, preventing further agglomeration of the NPs. For polyoxotungstates (POT), a suitable approach to enhance antibacterial activity is to combine 3d metal ions such as  $\text{Ti}(\text{IV})$ -containing species with lacunary POMs which act as polydentate O-donor ligands. In contrast with POTs, the use of lacunary polyoxomolybdate (POMo) ligands is limited because of their high instability in solution and their kinetically fast rearrangement reactions. In this regard, the  $[\text{Ti}_2(\text{HGeMo}_7\text{O}_{28})_2]^{10-}$  cluster, as the fourth water-soluble  $\text{Ti}(\text{IV})$ -containing POMo known to date, acts as a stabilizing ligand for the photo-assisted preparation of monodispersed metallic Au NPs ( $\text{Au}@\text{GeMoTi}$ ). The main bactericidal mechanism is mediated by cell membrane damage as the bacteria morphology, changes in the membrane polarization and release of nucleic acids confirm. The sub cytotoxic concentration of  $\text{Au}@\text{GeMoTi}$  for mouse mesenchymal stem cells (mMSCs) and U251MG was  $200\text{ }\mu\text{M}$ , but  $150\text{ }\mu\text{M}$  in macrophage and cultures of fibroblast. These values were much larger for minimum inhibitory concentration (MIC) and

minimum bactericidal concentration (MBC) values determined for *E. coli*.<sup>45</sup>

In another study, two Keggin-type POM anions,  $[\text{TiW}_{11}\text{CoO}_{40}]^{8-}$  ( $\text{TiW}_{11}\text{Co}$ ) and  $[\text{Ti}_2\text{PW}_{10}\text{O}_{40}]^{7-}$  ( $\text{Ti}_2\text{PW}_{10}$ ), have been prepared, which exhibited broad-spectrum activity against human respiratory pathogens such as coronavirus, rhinovirus, respiratory syncytial virus, and adenovirus. For example,  $\text{Ti}_2\text{PW}_{10}$  acts as an entry inhibitor against these viruses, effectively obstructing viral entry into host cells by blocking the interaction between the Spike protein of the virus and the cell receptor.  $\text{Ti}_2\text{PW}_{10}$  displayed an ability to inhibit the infectivity of RSV-A2, HCoV-OC43, HRV-A1, and AdV-5 viruses with excellent half maximal effective concentration ( $\text{EC}_{50}$ ) values of 0.65 to 3.30  $\mu\text{M}$  and highly favorable cytotoxic concentrations 50% ( $\text{CC}_{50}$ s) > 2400  $\mu\text{M}$  on different cell lines. These compounds do not encourage the development of resistant viral strains and have exhibited cytocompatibility, making them appealing for therapeutic applications. Its efficacy and nontoxicity to human cells make  $\text{Ti}_2\text{PW}_{10}$  a potential candidate for drug development against respiratory viral infections.<sup>46</sup>

### 3. POM-based biohybrids

POM-based materials have great potential for isolating proteins with notable selectivity. The anionic nature of the POM contributes a guiding effect by preferentially interacting with positively charged areas on the protein surface. In addition to electrostatic interactions, the non-covalent association between POMs and proteins is predominantly influenced by hydrogen bonding. The abundance of terminal and bridging oxygen atoms on the surface of POMs offers numerous sites for hydrogen bonding interactions with amino acid side chains.<sup>47</sup>

Recent investigations have illustrated the capabilities of POMs in fabricating separation membranes that can distinguish between small molecules, NPs, and proteins.<sup>48</sup> Covalent binding to biomolecules allows for the development of organic-inorganic hybrid materials from POMs. For promoting supramolecular self-assembly in solution, the bis-functionalized manganese hexamolybdate with an Anderson-Evans structure,  $\delta\text{-}[\text{MnMo}_6\text{O}_{18}\{\text{(OCH}_2)_3\text{C-R}\}_2]^{3-}$  (AER), is particularly compelling as it can be used to modulate POM-protein interactions and create POM-peptide self-assemblies possessing POD and antibacterial properties. Biotin-functionalized AER serves as an ideal component that can trigger the spontaneous self-assembly of streptavidin (SAv) into hybrid supramolecular POM-linked protein networks.<sup>49</sup>

In another example, two distinct POMs, ammonium heptamolybdate ( $(\text{NH}_4)_6\text{Mo}_7\text{O}_{24}$ ; AHM) and phosphotungstic acid ( $\text{H}_3\text{PW}_{12}\text{O}_{40}$ ; PWA), were incorporated into hydrogel beads derived from chitosan, referred to as chitosan/methylcellulose and chitosan/gelatin, respectively. The introduction of negatively charged POMs facilitates cross-linking among the positively charged chitosan chains *via* electrostatic interactions.

$[\text{Mo}_7\text{O}_{24}]^{6-}$  and  $[\text{PW}_{12}\text{O}_{40}]^{3-}$  serve as potent cross-linkers between chitosan chains possessing  $\text{NH}_3^+$  groups within their structure promoting the formation of hydrogel beads through electrostatic interactions. Furthermore, gelatin has a variety of polar groups capable of establishing hydrogen bonds with moieties present on the chitosan chains, including carboxylic acid ( $-\text{COOH}$ ), amine ( $-\text{NH}_2$ ), and hydroxyl ( $-\text{OH}$ ) functional groups. The incorporation of POMs within the biopolymer hydrogel beads substantially enhanced their antibacterial efficacy against *E. coli*, as well as *S. aureus*. The presence of a hydrogel matrix as a host supports adsorption at a cellular level and reduces the toxicity of pure POMs. The interaction between POMs and the flavin mononucleotide (FMN) species in the cell's mitochondria leads to the formation of a complex that prevents electron transfer from nicotinamide adenine dinucleotide (NADH) to co-enzyme Q10, causing severe damage to the normal metabolism of the bacterial cells. This interference disrupts the transport mechanisms across the bacterial cell wall, adversely influencing the conventional energy production pathways and resulting in elevated levels of ROS. On the other hand, anticancer activity was displayed against HeLa cells *in vitro* cytotoxicity of 85% for loaded hydrogel beads with AHM and 70% for loaded hydrogel beads with PWA.<sup>50</sup>

In another study, the formation of a supramolecular hydrogel based on Keggin-type POMs ( $\text{PW}_{12}\text{O}_{40}^{3-}$ ; PTA and  $\text{SiW}_{12}\text{O}_{40}^{4-}$ ; STA) with guanosine monophosphate (GMP) was reported as an efficient artificial haloperoxidase mimic to catalyze halide ion ( $\text{X}^-$ ) oxidation in the presence of  $\text{H}_2\text{O}_2$ . The results of this study showed that the formation of POM-based hydrogels leads to a multi-fold increase in biocompatibility and mechanical strength for antifouling activities. Compared to the pure POM solution, the  $\text{IC}_{50}$  values of STA-GMP and PTA-GMP hydrogels against HEK 293 cell lines demonstrated an increase of 4.1 and 3.7 times, respectively. In the presence of the PTA-GMP hydrogel along with  $\text{H}_2\text{O}_2$  and NaI, the results of antibacterial performance demonstrated bacterial growth reduction for *B. subtilis* and *E. coli* by 99.9% compared to pure PTA solution (94% for *B. subtilis* and 80% for *E. coli*).<sup>51</sup>

Establishing interactions between POM and the enzyme to immobilize it and increase its biocatalytic performance has been another topic of interest. For example,  $\text{H}_3\text{PW}_{12}\text{O}_{40}@\text{UiO}-67$  was employed as a sorbent for microperoxidase (MP-11) enzyme encapsulation. Hydrogen bonding and electrostatic interactions with  $\text{PW}_{12}\text{O}_{40}^{3-}$  could encapsulate the enzyme and increase biocatalytic performance, avoiding enzyme aggregation and leaching.<sup>52</sup> The activity of distributed POMs within MOFs, combined with their porosity and high surface area, significantly enhances enzyme immobilization.

Developing POMs that are stable at near neutral pH has been of interest for their potential as membrane carriers. Thus, a new biological system in neutral physiological media, characterized by the use of mixed-metal Keggin POMs (Fig. 7a), exhibited stable properties and facilitated the membrane transport of impermeable, hydrophilic, and cationic

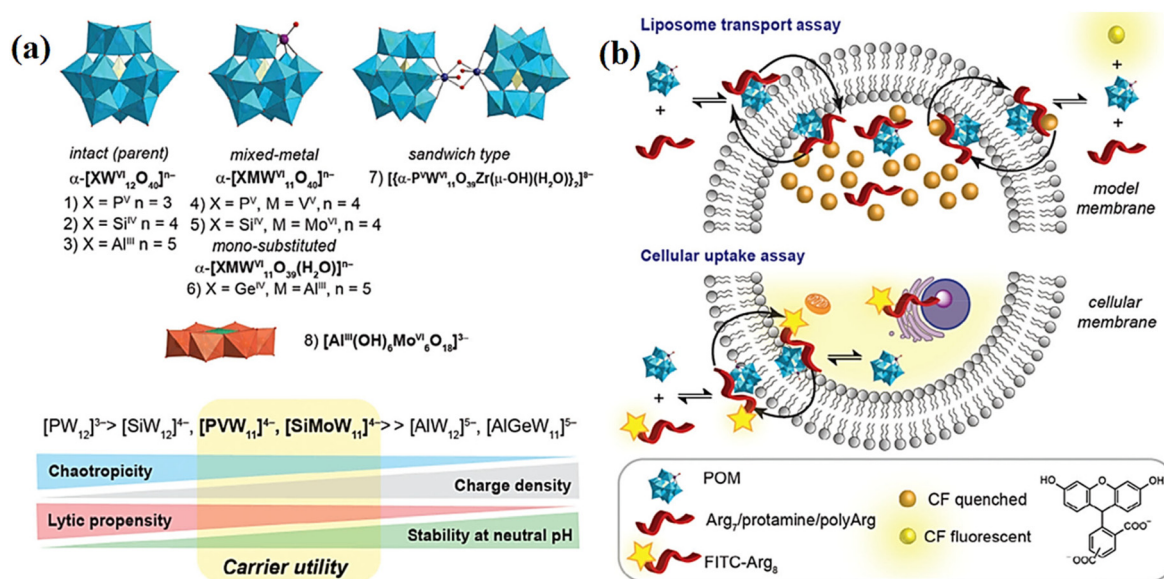


**Fig. 7** (a) Schematic illustration of the investigated POMs categorized by their chaotropic character based on charge density, experimentally determined pH stability, and predicted membrane lytic potential. (b) Schematic illustration of an impermeable oligopeptide transported by POMs in model and cellular membranes. Adapted with permission from ref. 53. Copyright 2024 Wiley.

peptides such as heptalysine, heptaarginine, protamine, and polyarginine. The observed uptake in both model membranes and cells is attributed to the superchaotropic properties and supramolecular interactions driven by electrostatic interactions between POM and cationic peptides (Fig. 7b). The results suggest that POM carriers should be optimized to reduce their cellular toxicity while preserving their hydrolytic stability.<sup>53</sup>

Within the expanded realm of POM applications in biological methods, it could also refer to their adoption in a biology-inspired artificial intelligence (AI) concept. For this purpose, a functional metal–DNA-modified Lindqvist-type polyoxovanadate (POV6) was prepared to simulate the activity of an artificial synapse, wherein DNA origami acts as a carrier framework and is anchored onto an Au substrate. In the POV6–DNA composite, the method of stepwise charge modulation enables low-energy resistive switching and synaptic-like behavior by controlling the mechanism of electron transfer in the composite. The POV6 species are capable of accepting electrons gradually, enabling them to replicate synaptic behavior. This ability allows them to adjust their state depending on the number of electrons accepted, similar to how biological synapses regulate their strength through neurotransmitter release.<sup>54</sup> The development of such research can significantly contribute to the growth of POM-based hybrids for biocompatible complementary metal oxide semiconductor (CMOS) technology.

The integration of POMs with biomolecules enhances biocompatibility, therapeutic efficacy, and target specificity. Despite the current focus on certain biomolecules such as amino acids, peptides, *etc.* in the literature on POM-based biohybrids, the potential of other biomolecules warrants further investigation.

## 4. Conclusions and perspectives

In this study, we highlighted recent progress in the potential of POM-based materials in therapeutic and biomedical applications. The role of surface charge, redox activity, pH-sensitive aggregation behavior, and the creation of a variety of non-covalent interactions as well as biocompatibility improvement in POMs exhibit substantial potential for efficient biomedicine activities. POM-based materials also exhibit significant potential as radiation therapy sensitizers, increasing the sensitivity of tumor cells to radiation and thereby enhancing the effectiveness of radiation therapy. The achievement of this aim can be effectively integrated with PDT and PTT by employing nanobots.

The biomedical potential of POM-based materials will be significantly reduced if they don't exhibit catalytic activity under regular physiological conditions and are not biodegradable. Therefore, understanding the metabolic pathways of these materials in the body is crucial to ensure their safe decomposition and controlled elimination.

The existence of different conditions of target cells in the biological environments, external stimulating agents, and the diverse role of POMs that can exhibit prominent catalytic activity (*e.g.* POD-like, GSH/POD-like, *etc.*) through the production of ROS to inhibit tumor growth. Some biological environments allow them to scavenge excess ROS *via* serine protease and SOD activities or their inherent redox characteristics, thereby preventing cellular damage.

Based on the perspective of bioorthogonal chemistry, POM-based materials should be inert within biological media while simultaneously displaying reactivity towards specific substrates. There is an important need to make POMs specific to



target cells and with the inherent toxicity of POMs, it is important to evaluate toxicity consequences in cells when complexed or unmodified POMs enter non-targeted cells. To reverse such a challenge, one can encapsulate POMs in porous materials or apply organic modifications to minimize toxicity toward healthy tissue and improve safety.

The evolution of biotechnology trends such as targeted drug delivery (encompassing modification, *in situ* drug assembly, release control, *etc.*), *in vivo* imaging and cell labeling, and the development of biocompatible switchable POM species at neuron–cell interfaces, *etc.* could be useful towards the development of the concept of bioorthogonal chemistry of POMs. Also, the use of rare earth elements to modify POMs as luminescent probes/sensors enables the monitoring of POM-based materials' metabolism and accumulation into cellular media. This approach facilitates visual sensing of these processes at the subcellular level.

Addressing synthetic challenges of POM-based biohybrids and their stability within biological media must consider limiting factors in the use of these materials, which depend on several variables (including temperature, pH, time, precursor amounts, *etc.*). Thus, studies must be expanded not only to explore new ways of biohybrid synthesis, but also to better understand their changes in solution over time, particularly under different biologically relevant conditions, to optimize their design.

Despite the promising applications in therapeutic and biomedicine of POM-based materials, their transposition to clinical environments is still in the early stages, with current research classified at technology readiness levels (TRLs) at TRL 3 to TRL 5. Significant challenges remain in optimizing their pharmacokinetics, toxicity profiles, and large-scale production for clinical applications. As researchers systematically address these challenges, POMs have considerable potential to enhance therapeutic strategies in modern biomedicine.

## Author contributions

Milad Moghadas: writing – original draft, project administration, and writing – review & editing. Mohammad Abbasi and Mahtab Mousavi: investigation and writing – original draft. Masoud Mirzaei: writing – review & editing and supervision.

## Data availability

No primary research results, software, or codes have been included and no new data were generated or analyzed as part of this review.

## Conflicts of interest

The authors declare no conflict of interest.

## Acknowledgements

The authors express gratitude for the support of Ferdowsi University of Mashhad (FUM) and the Iran Nanotechnology Innovation Council (INIC).

## References

- 1 G. Paramasivam, A. Sanmugam, V. V. Palem, M. Sevanan, A. B. Sairam, N. Nachiappan, B. Youn, J. S. Lee, M. Nallal and K. H. Park, *Int. J. Biol. Macromol.*, 2024, **254**, 127904.
- 2 T. Ma, R. Yan, X. Wu, M. Wang, B. Yin, S. Li, C. Cheng and A. Thomas, *Adv. Mater.*, 2024, **36**, 2310283.
- 3 Y. Song, Y. Sun, M. Tang, Z. Yue, J. Ni, J. Zhao, W. Wang, T. Sun, L. Shi and L. Wang, *ACS Appl. Mater. Interfaces*, 2022, **14**, 4914–4920.
- 4 M. Yang, J. Li, K. Hui, J. Ying and A. Tian, *Dalton Trans.*, 2024, **53**, 15412–15420.
- 5 L. Wang, P. Dai, H. Ma, T. Sun and J. Peng, *Inorg. Chem. Front.*, 2024, **11**, 1339–1365.
- 6 S. K. Petrovskii, E. V. Grachova and K. Yu. Monakhov, *Chem. Sci.*, 2024, **15**, 4202–4221.
- 7 D. E. Salazar Marcano and T. N. Parac-Vogt, *Coord. Chem. Rev.*, 2024, **518**, 216086.
- 8 K. Dashtian, S. Shahsavarifar, M. Usman, Y. Joseph, M. R. Ganjali, Z. Yin and M. Rahimi-Nasrabadi, *Coord. Chem. Rev.*, 2024, **504**, 215644.
- 9 Z. Khoshkhan, M. Mirzaei, A. Amiri, N. Lotfian and J. T. Mague, *Inorg. Chem.*, 2024, **63**, 2877–2887.
- 10 M. Babaei Zarch, M. Mirzaei, M. Bazargan, S. K. Gupta, F. Meyer and J. T. Mague, *Dalton Trans.*, 2021, **50**, 15047–15056.
- 11 X. Xu, Y. Guo, B. Li, Y. Lv, Z. Wu, S. Liang, L. He and Y.-F. Song, *Coord. Chem. Rev.*, 2025, **522**, 216210.
- 12 J. Chen, W.-Z. Yang, H. Chen, X. Ding, H. Chen, C.-H. Zhan and Z. Jin, *Inorg. Chem. Front.*, 2024, **11**, 7238–7255.
- 13 X. Liu, T. Sun, Y. Sun, A. Manshina and L. Wang, *Nano Mater. Sci.*, 2024, S2589965124000278, In Press.
- 14 Y. Zhang, Z. Cheng, B. Zeng, J. Jiang, J. Zhao, M. Wang and L. Chen, *Dalton Trans.*, 2024, **53**, 10805–10813.
- 15 M. Wang, L. Cui, K. Yu, Q. Wang, C. Guo and B. Zhou, *Appl. Surf. Sci.*, 2024, **653**, 159312.
- 16 J. Yao, J. Sun, X. Li, Y. Lin, Y. Zhao, X. Chen, M. Li, Z. Wang and Z.-M. Su, *J. Mol. Struct.*, 2025, **1319**, 139485.
- 17 J. Lu, X. Xu and J. Chen, *Microchim. Acta*, 2024, **191**, 544.
- 18 H. Khan, J. Yang, M. Wang, J. Sun, H. Zhang and L. Yang, *Chem. Eng. J.*, 2024, **499**, 156129.
- 19 G. Du, M. Lv, H. Wang, C. Liu, Q. Xu, J. Liu, Z. Yang, Y. Yong and Y. Han, *Nanoscale Adv.*, 2023, **5**, 3985–3993.
- 20 F. Chen, L. Hou, Y. Gao, J. Zhou, F. Kong, D. Han and W. Zhao, *Adv. Funct. Mater.*, 2024, 2408186.
- 21 K. Song, W. Zhao, Y. Zhou, D. Liu and P. K. Chu, *Coord. Chem. Rev.*, 2024, **520**, 216161.
- 22 M. Samaniyan, M. Mirzaei, R. Khajavian, H. Eshtiagh-Hosseini and C. Streb, *ACS Catal.*, 2019, **9**, 10174–10191.

- 23 B. Mohanty, S. Kumari, P. Yadav, P. Kanoo and A. Chakraborty, *Coord. Chem. Rev.*, 2024, **519**, 216102.
- 24 L. Gong, L. Chen, Q. Lin, L. Wang, Z. Zhang, Y. Ye and B. Chen, *Small*, 2024, **20**, 2402641.
- 25 L. Zhu, A. Huo, Y. Chen, X. Bai, C. Cao, Y. Zheng and W. Guo, *Chem. Eng. J.*, 2023, **476**, 146613.
- 26 Y. Chen, Y. Deng, Y. Li, Y. Qin, Z. Zhou, H. Yang and Y. Sun, *ACS Appl. Mater. Interfaces*, 2024, **16**, 21546–21556.
- 27 J.-W. Lin, Y. Zhou, H.-P. Xiao, L.-L. Wu, P.-C. Li, M.-D. Huang, D. Xie, P. Xu, X.-X. Li and Z.-X. Li, *Chem. Sci.*, 2024, **15**, 15367–15376.
- 28 C. Liu, M. Lv, Q. Xu, J. Xie, Y. You, K. Guo, G. Jiang, L. Hou, H. Yang and Y. Yong, *Nano Today*, 2024, **58**, 102415.
- 29 A. G. Kurian, N. Mandakhbayar, R. K. Singh, J.-H. Lee and H.-W. Kim, *ACS Appl. Mater. Interfaces*, 2024, **16**, 34641–34655.
- 30 C. Wang, Z. Dai, Q. Zhang, X. Li, M. Ma, Z. Shi, J. Zhang, Q. Liu and H. Chen, *Chem. Eng. J.*, 2024, **490**, 151601.
- 31 J. F. Ramirez Henao, S. Boujday, C. Wilhelm, B. Bouvet, S. Tomane, I. Christodoulou, D. Sun, G. Cure, F. B. Romdhane, A. Miche, A. Dolbecq, P. Mialane and A. Vallée, *ACS Appl. Nano Mater.*, 2024, **7**, 21094–21103.
- 32 F. Yang, Y. Chen, Y. Xiao, H. Jiang, Z. Jiang, M. Yang, M. Li, Y. Su, Z. Yan, Y. Lin and D. Li, *Pharmacol. Res.*, 2023, **188**, 106645.
- 33 Z. Tao, J. Wang, H. Wu, J. Hu, L. Li, Y. Zhou, Q. Zheng, L. Zha and Z. Zha, *ACS Appl. Mater. Interfaces*, 2023, **15**, 11474–11484.
- 34 B. Li, Z. Wu, X. Xu, Y. Lv, Y. Guo, S. Liang, Z. Wang, L. He and Y.-F. Song, *Inorg. Chem. Front.*, 2024, **11**, 4439–4448.
- 35 D. Wang, Z. Tang, W. Zhang, Y. Chen, L. Chen, S. Song and J. Zhao, *Small*, 2024, 2405068.
- 36 Y. Zhao, C.-L. Li, C.-Q. Chen, J. Du, U. Kortz, T. Gong and P. Yang, *Inorg. Chem. Front.*, 2024, **11**, 1413–1422.
- 37 T. Ma, X. Ma, Z. Lin, J. Zhang, P. Yang, T. Csúpász, I. Tóth, S. Misirlic-Dencic, A. M. Isakovic, D. Lembo, M. Donalisio and U. Kortz, *Inorg. Chem.*, 2023, **62**, 13195–13204.
- 38 B. Li, X. Xu, Y. Lv, Z. Wu, L. He and Y. Song, *Small*, 2024, **20**, 2305539.
- 39 M. Babaei Zarch, M. Bazargan and M. Mirzaei, *Inorg. Chem.*, 2024, **63**, 6141–6151.
- 40 Q. Huo, C. Chen, J. Liao, Q. Zeng, G. Nie and B. Zhang, *Biomaterials*, 2024, **311**, 122665.
- 41 M. Tang, J. Ni, Z. Yue, T. Sun, C. Chen, X. Ma and L. Wang, *Angew. Chem., Int. Ed.*, 2024, **63**, e202315031.
- 42 M. Ma, Z. Liu, H. Zhao, H. Zhang, J. Ren and X. Qu, *Natl. Sci. Rev.*, 2024, **11**, nwae226.
- 43 Y. Wang, Z. Yu, J. Xiong, K. Yan and X. Lu, *Adv. Funct. Mater.*, 2024, **34**, 2405880.
- 44 N. Song, M. Lu, J. Liu, M. Lin, P. Shangguan, J. Wang, B. Shi and J. Zhao, *Angew. Chem., Int. Ed.*, 2024, **63**, e202319700.
- 45 M. Paesa, F. Almazán, C. Yus, V. Sebastián, M. Arruebo, L. M. Gandía, S. Reinoso, I. Pellejero and G. Mendoza, *Small*, 2024, **20**, 2305169.
- 46 I. Arduino, R. Francese, A. Civra, E. Feyles, M. Argenziano, M. Volante, R. Cavalli, A. M. Mougharbel, U. Kortz, M. Donalisio and D. Lembo, *Antiviral Res.*, 2024, **226**, 105897.
- 47 S. Lentink, D. E. Salazar Marcano, M. A. Moussawi and T. N. Parac-Vogt, *Angew. Chem., Int. Ed.*, 2023, **62**, e202303817.
- 48 G. Zhang, X. Li, G. Chen, Y. Zhang, M. Wei, X. Chen, B. Li, Y. Wu and L. Wu, *Nat. Commun.*, 2023, **14**, 975.
- 49 D. E. Salazar Marcano, S. Lentink, J. Chen, A. V. Anyushin, M. A. Moussawi, J. Bustos, B. Van Meerbeek, M. Nyman and T. N. Parac-Vogt, *Small*, 2024, **20**, 2312009.
- 50 A. Shaheen, P. Kour, U. N. Tak, H. A. Mir, G. Ahanger, S. Sidiq and A. A. Dar, *ACS Appl. Eng. Mater.*, 2024, **2**, 1706–1723.
- 51 A. Chakraborty, S. Dash, N. Thakur, V. Agarwal, D. Nayak and T. K. Sarma, *Biomacromolecules*, 2024, **25**, 104–118.
- 52 Q. An, Z. Xu, W. Shang, Y. Wang, X. Liu, D. Guo, M. Zeng and Z. Jia, *ACS Appl. Bio Mater.*, 2022, **5**, 1222–1229.
- 53 A. Barba-Bon, N. I. Gumerova, E. Tanuhadi, M. Ashjari, Y. Chen, A. Rompel and W. M. Nau, *Adv. Mater.*, 2024, **36**, 2309219.
- 54 E. Vogelsberg, M. Moors, A. S. Sorokina, D. A. Ryndyk, S. Schmitz, J. S. Freitag, A. V. Subbotina, T. Heine, B. Abel and K. Yu. Monakhov, *Chem. Mater.*, 2023, **35**, 5447–5457.